

# Investigation of Microwave Transducers for Linearity Dependence and Applications in Quantum Networking

Summer Bolton<sup>a&</sup>, Joseph M. Lukens<sup>b\*</sup>, Carson Moseley<sup>a</sup>, Maddy Woodson<sup>c</sup>, Steven Estrella<sup>c</sup>,  
Shunqiao Sun<sup>a</sup>, Seongsin M. Kim<sup>a</sup>, and Patrick Kung<sup>a§</sup>

<sup>a</sup>Electrical and Computer Engineering, The University of Alabama, Tuscaloosa, AL 35487;

<sup>b</sup>Quantum Information Science Section, Oak Ridge National Laboratory, Oak Ridge, TN 37831;

<sup>c</sup>Freedom Photonics, Santa Barbara, CA 93117

## ABSTRACT

Quantum devices have the potential to revolutionize applications in computing, communications, and sensing; however, current state-of-art resources must operate at extremely low temperatures, making the routing of microwave control and readout signals challenging to scale. Interest in microwave photonic solutions to this problem has grown in recent years, in which control signals are delivered to the cold stage via optical fiber, where they are converted to electrical signals through photodetection. Overall link performance depends strongly on the characteristics of the photodiode, yet detailed measurements of many detector properties remain lacking at cold temperatures. In this work, we examine and compare the performance of a modified uni-traveling carrier photodiode (MUTC-PD) at both room (300 K) and liquid nitrogen (80 K) temperatures, focusing in particular on responsivity, bandwidth, and linearity. In line with previous work, we find a sharp reduction in responsivity at 1550 nm as temperature decreases, while RF bandwidth remains steady. Interestingly, our linearity tests reveal that the RF output saturates more quickly at 80 K, suggesting reduced linearity with lower temperature, the cause of which is still under investigation. Our results should help contribute to the understanding and future design of highly linear cryogenic quantum links.

**Keywords:** MUTC-PD, quantum devices, RF photonics, linearity, cryogenic quantum links

## 1. INTRODUCTION

Given the variety of technologies currently being explored for quantum computing, it is expected that quantum networks—infrastructures that transmit quantum information and establish entanglement between distributed quantum resources—will need to support an array of heterogenous systems [1]. Many of these platforms, such as superconducting circuits [2] and silicon qubits [3], rely on precise microwave control pulses and sequences for the realization of high-fidelity quantum gates. Yet their required operating temperatures ( $<1$  K) present two major challenges for scaling to many qubits: first, blackbody radiation introduces a significant thermal load in the microwave domain, thereby demanding heavy RF attenuation between stages in a dilution refrigerator; second, as the number of qubits grows, so does the number of required coaxial cables, which are in turn ultimately limited by the fridge dimensions [4].

Microwave photonics [5,6] offers the potential to address both limitations, by using microwave control signals to modulate optical fields at room temperature, delivering these photonic waveforms to the cold stage via optical fiber, and there converting the optical waveforms back to microwave signals on a fast photodiode. The reduced thermal load at optical wavelengths, coupled with parallelization through wavelength-division multiplexing, can in principle support orders of magnitude more qubits in a single fridge than possible with coaxial cable. A seminal recent experiment has highlighted the feasibility of this approach in the context of a transmon superconducting qubit [7].

Link performance for qubit control with microwave photonics will depend heavily on the photodiode's ability to realize optical-to-electrical (OE) conversion with high efficiency, wide bandwidth, and high linearity at ultracold temperatures.

---

This manuscript has been co-authored by UT-Battelle, LLC, under contract DE-AC05-00OR22725 with the US Department of Energy (DOE). The US government retains and the publisher, by accepting the article for publication, acknowledges that the US government retains a nonexclusive, paid-up, irrevocable, worldwide license to publish or reproduce the published form of this manuscript, or allow others to do so, for US government purposes. DOE will provide public access to these results of federally sponsored research in accordance with the DOE Public Access Plan (<http://energy.gov/downloads/doe-public-access-plan>).

\*lukensjm@ornl.gov; phone 865-241-5070; §patkung@eng.ua.edu; phone 205-348-1763; &current affiliation: Draper Laboratory, Cambridge, MA

Previous investigations into cryogenic OE conversion for both p-i-n [8] and uni-traveling carrier [9–12] photodiodes have generally confirmed the preservation of high RF bandwidth down to few-kelvin temperatures, with reduced responsivity in the C-band (1530–1570 nm) due to bandgap widening in InGaAs. Linearity is likewise a critical feature of photodetectors in analog photonics; a highly linear photodiode is able to implement OE conversion in which the output photocurrent is a scaled replica of the input optical power with minimal distortion [13]. However, detailed studies of photodiode linearity at cryogenic temperatures have so far been few [14], leaving an important gap in the continued development of ultracold microwave photonic links.

In this work, we test a modified uni-traveling carrier photodiode (MUTC-PD) designed for high saturation currents at both 300 K and 80 K. After confirming low dark current and a responsivity that drops as expected with temperature, we probe RF bandwidth with an optical heterodyne setup comprising two lasers with detuned frequencies. Bandwidth does not vary with temperature, but significantly with bias voltage in agreement with expectations. Finally, we use an erbium-doped fiber amplifier (EDFA) to increase incident optical power up to ~20 dBm, measuring the RF output at test frequencies of 3 GHz and 10 GHz. Up to our maximum optical power levels, no appreciable compression is observed under –5 V bias; for zero bias, however, the 1 dB compression points are perceptibly lower at 80 K compared to 300 K. Further research will be required to understand the interplay between thermal and responsivity effects and explore performance down to much colder sub-kelvin temperatures. Overall, our results provides an important glimpse into highly linear photodiodes for emerging applications in quantum networking.

## 2. EXPERIMENTAL METHODS

### 2.1 MUTC-PD

A modified uni-traveling carrier photodiode (MUTC-PD) is a unique photodiode architecture which enables the design of high-bandwidth photodiodes which saturate at high levels of input optical power, building off the uni-traveling carrier photodiode (UTC-PD). A traditional UTC-PD employs a doped absorber which generates electron-hole pairs. The electrons move into a wider-bandgap collector layer, which is depleted with appropriate reverse bias, and the electrons accelerate through this layer to be collected at the n-contact. A wide-bandgap barrier layer blocks electron diffusion to the p-contact. Meanwhile, the holes generated through optical absorption are collected immediately (hence the term “uni-traveling” carrier). An MUTC-PD leverages the UTC-PD structure, with some improvements to further combat electric field collapse through the space-charge effect, as well as a modification to the absorber such that it is partially depleted (i.e. both a p-doped layer and an unintentionally doped layer). Figure 1 shows a representative band diagram (a) and device structure (b) for an MUTC-PD of the form used in the tests here.

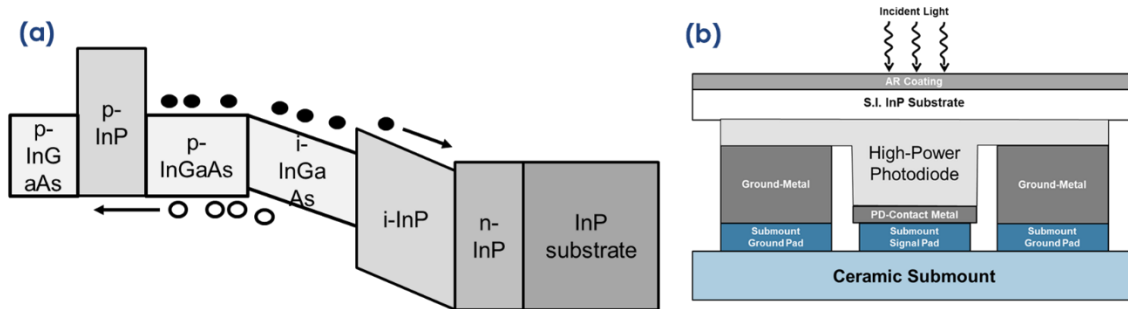


Figure 1. (a) Simplified illustrated band diagram of an MUTC-PD structure and (b) cross-section of a backside-illuminated, high-power MUTC-PD bonded to a ceramic submount.

### 2.2 Optical Heterodyning Principle

The heterodyne beat method is used to mix slightly detuned lasers, as shown in Fig. 2. Two fiber-coupled lasers in the C-band are brought into the same linear polarization state by feeding each through a polarization controller. The optical signals are then combined in a single-mode fiber coupler before being fed through a single-mode polarizer. LaserF is configured at a fixed wavelength of 1536 nm (195.17 THz), while LaserT is tunable between from 1525 to 1570 nm (191.5 to 186.5 THz). A fast MUTC-PD is connected to the polarizer and acts as a transducer that will convert the mixed the laser beams into a microwave signal.

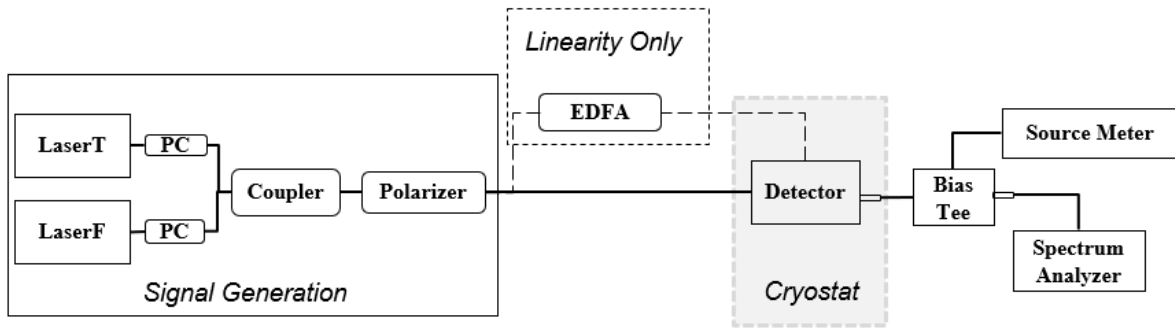


Figure 2. Block diagram of test setup for cryogenic photodetector characterization using the heterodyne beat method. An EDFA is to increase incident optical power for the linearity tests.

### 2.3 Experimental Photodiode Characterization

The experimental setup used to characterize the devices is shown in Fig. 2. The fiber pigtailed MUTC-PD is mounted inside a cryostat. A fiber patch cord carries the laser signal after the polarizer to a vacuum-tight fiber feedthrough. The detector is electrically connected to an RF cable that is connected to a bias tee via an RF feedthrough. The pure RF signal is sent to a spectrum analyzer while a source meter is used to provide the detector DC bias.

The dark current-voltage characteristics of the MUTC-PD are measured using the source meter from  $-5.0$  to  $+0.5$  V bias at 300 and 80 K. The DC spectral responsivity measurements are carried out using LaserT only, in the range from 1525 to 1570 nm (approximately 197 to 191 THz). The input optical power to the device is measured after the polarizer using a calibrated power meter. The optical power of the LaserT is recorded using a calibrated power meter while the DC current is recorded using the source meter.

The frequency response characterizes the available RF bandwidth of the device in use, which is important for high-frequency applications. The experimental setup for measuring the frequency response is shown in Fig. 2 (excluding the dashed box). The polarizer is connected to a cryostat feedthrough using a fiber patch cord. Inside the cryostat are the photodetector being tested and cables connecting it to the exterior. A bias tee is connected to the output of the detector; it is biased with a source meter that also measures the DC current. The RF response is observed using a spectrum analyzer. This system remains the same regardless of the desired temperature; for cold temperature testing, the cryostat is filled with liquid nitrogen until the detector reaches 80K. In order to maximize modulation efficiency, the powers of both lasers are matched as close as possible after the polarizer. Then the polarizer is connected to the cryostat to begin the experiment. A bias voltage of either  $-5$  V or  $0$  V is applied to the bias tee. LaserF is set to 1536 nm and remains unchanged throughout the experiment while LaserT is initially set to a detuning of  $\sim 2$  GHz from LaserF. From the spectrum analyzer, the RF power and frequency are recorded. LaserT is incremented in units of 2 GHz and the process repeats for the full range of the spectrum analyzer, typically 27 GHz. This frequency response is measured at  $-5$  V and  $0$  V bias and at temperatures of 300 K and 80 K.

The linearity of a photodetector as a function of excitation power is important to ensure faithful OE conversion and to minimize harmonic distortion [6,13]—of particular relevance for the types of analog photonic signals envisioned in cryogenic quantum links. The experimental setup remains as in Fig. 2, with the addition of an EDFA between the polarizer and the optical fiber feedthrough. The optical power is measured after the EDFA using a calibrated power meter, while the RF power and frequency are measured on the spectrum analyzer as the EDFA pump current is gradually increased. We focus on performance at two RF frequencies, 3 GHz and 10 GHz. Again, measurements are performed at 300 and 80 K, and for a DC bias of  $-5$  and  $0$  V.

### 3. RESULTS AND DISCUSSION

#### 3.1 Temperature-Dependent Spectral Responsivity

Figure 3(a) shows the dark current measured at 300 K and 80 K. Under reverse bias (the designed operating point), dark current is  $\sim 5$  nA, for both temperatures. (The discontinuity at 0 V is an artifact resulting from rescaling on the source meter.) The frequency-dependent responsivity appears in Fig. 3(b), which was calculated by dividing the output DC photocurrent by the independently measured input optical power ( $\sim 6.5$  mW in this test). The responsivity is flat in the entire band of interest at 300 K. At 80 K, the responsivity reduces overall and shows a clear downward trend with increasing wavelength. This behavior can be attributed to band gap widening at lower temperatures and is consistent with previous investigations [9].

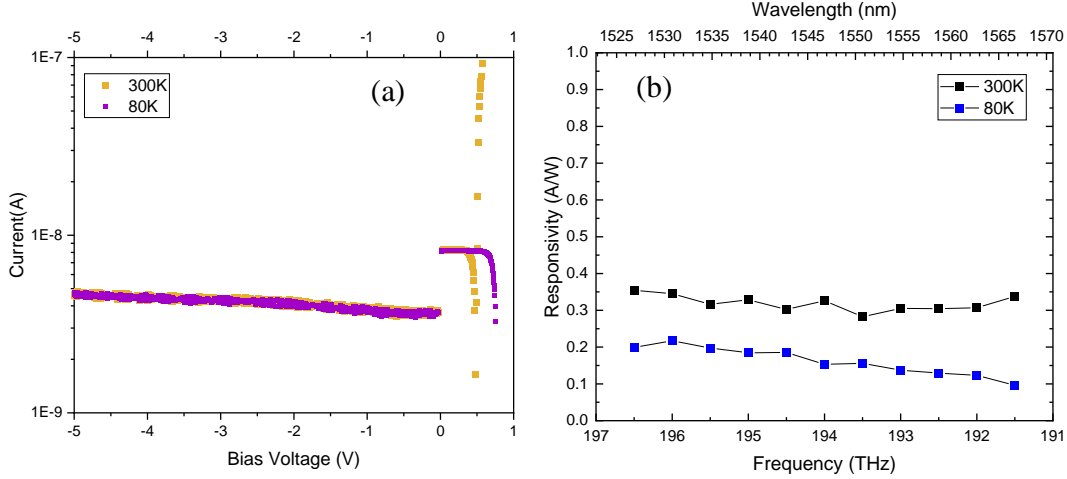


Figure 3. (a) Bias-voltage-dependent dark current at 300 K and 80 K. (b) Responsivity versus optical frequency for 300 K and 80 K.

#### 3.2 RF Bandwidth

The RF frequency response is measured using the full heterodyne setup of Fig. 2, by scanning the difference frequency between the two lasers. Results shown in Fig. 4 were obtained with total input optical power of 11 mW. In order to compare all configurations on a similar scale, we normalize the RF power in each curve to its value at the lowest frequency, which removes any variations from responsivity [Fig. 3(b)]; similarly, we back out the frequency response of the measurement system so that the plots reflect only the MUTC-PD under test. For  $-5$  V bias, the 3 dB bandwidth is approximately 20 GHz, which is consistent with previous measurements with similar devices at room temperature [15]. At 0 V bias, the 3 dB bandwidth reduces to approximately 6 GHz at both temperatures. The similarities between the curves at 300 K and 80 K confirm that this MUTC-PD preserved RF bandwidth as temperature reduces, in line with previous findings of constant RF bandwidth with temperature for p-i-n photodiodes [8]. We do note that, as evident by the reduced bandwidth at 0 V, the zero bias condition is highly non-optimal for this detector. Nonetheless, we find it extremely useful to consider, for two main reasons: (i) at 0 V bias, one could potentially reduce the thermal load from resistive heating at cold temperatures; and (ii) this operating point allows us to push the photodiode into deep saturation, valuable for the linearity tests in the next section.

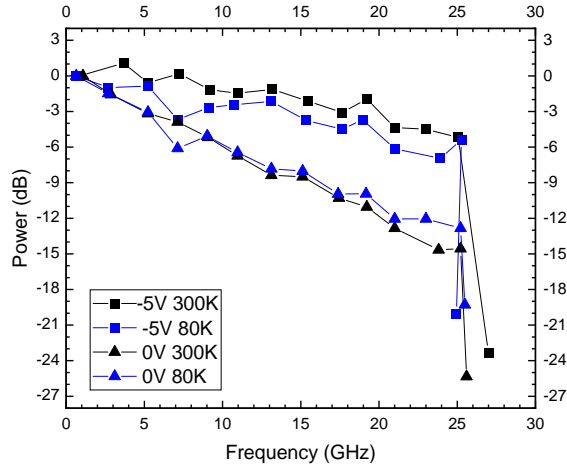


Figure 4. Frequency response (normalized) for  $-5$  V and  $0$  V bias at  $300$  K and  $80$  K.

### 3.3 Frequency and Temperature Dependent Linearity and Compression of RF Photonics Link

The linearity results are shown in Fig. 5. Linearity is typically benchmarked against the ideal RF power obtainable with a perfect device and 100% temporal modulation contrast, i.e.,  $P_{\text{ideal}} = \frac{1}{2} Z I_D^2$ , where  $Z = 50 \Omega$  and  $I_D$  is the measured DC photocurrent;  $P_{\text{ideal}}$  is represented with solid black lines in the plots. The maximum value of  $I_D$  attainable experimentally depends on both the responsivity for the specific temperature and the incident optical power (up to  $\sim 20$  dBm with our EDFA). Accordingly,  $I_D$  is lower for  $80$  K than  $300$  K for all plots. All experimental curves lie below  $P_{\text{ideal}}$  as required, although their vertical offsets are not particularly meaningful, since these measurements were performed at different times and likely different optical power balancing of the two heterodyning lasers.

At  $-5$  V bias, no appreciable saturation is observed for any temperature or RF frequency. The  $1$  dB compression point for  $-5$  V applied voltage bias thus must exceed our maximum observations of  $45$  mA at room temperature and  $30$  mA for  $80$  K at the experimented conditions. Without any applied voltage bias, saturation is quickly observed, and a  $1$  dB compression point can be estimated. The highest  $1$  dB compression point for  $0$  V bias occurs at room temperature and  $10$  GHz while the lowest occurs at  $80$  K and a frequency of  $3$  GHz. Table 1 summarizes the results of linearity and the compression behavior at  $300$  K and  $80$  K.

Interestingly, we notice saturation at slightly lower photocurrents for  $80$  K compared to  $300$  K. Initially, we would have expected the opposite, since thermal damage should be mitigated by active cooling; indeed, previous tests of amplitude-to-phase nonlinearity in MUTCs found improved performance at reduced temperatures [14]. We conjecture that the lower saturation currents in our  $80$  K measurements might be caused by the lower responsivity, as the extra undetected optical power at  $80$  K could be contributing to localized heating in unpredictable ways. Further investigations into these effects are ongoing.

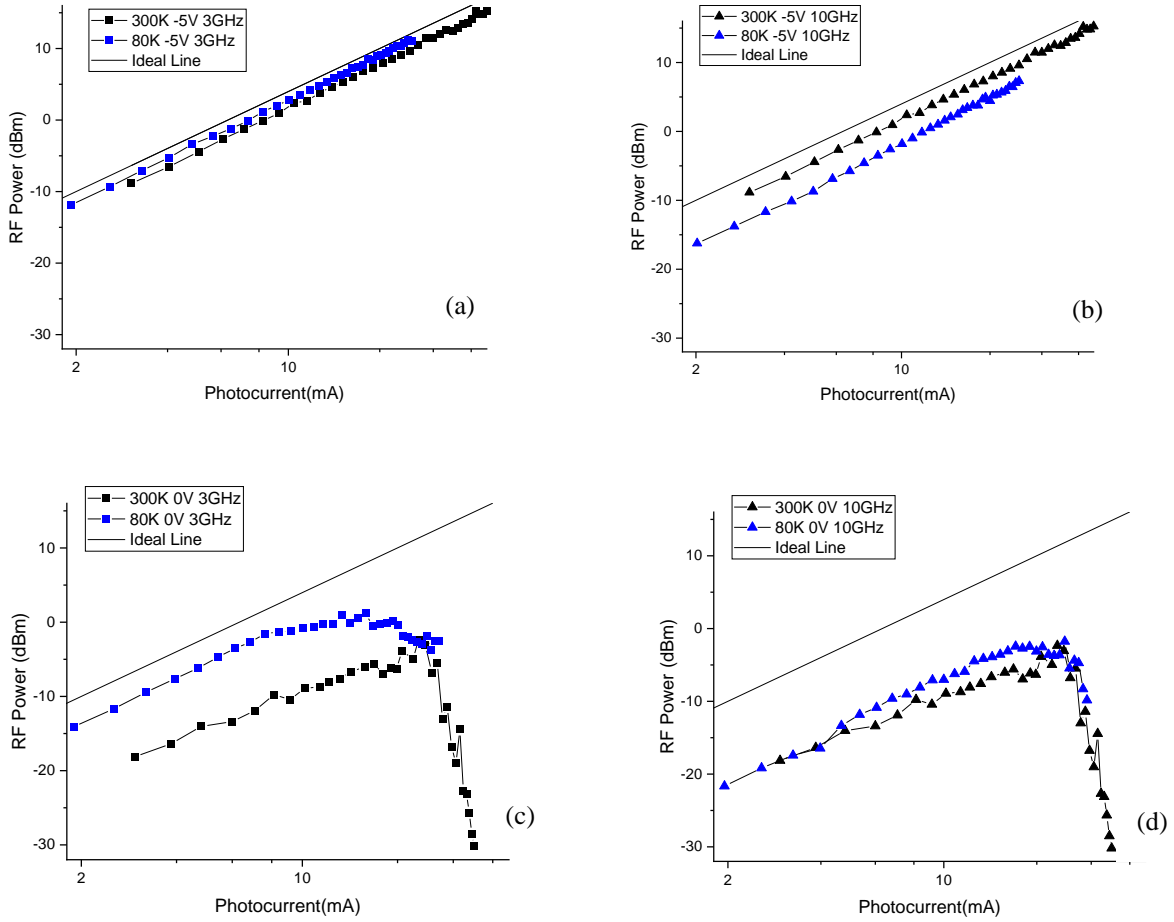


Figure 5. Linearity results comparing 300 K and 80 K at each tested parameter

Table 1. Saturation currents for the tested MUTC-PD at 300 K and 80 K.

	<b>300 K</b>	<b>80 K</b>
-5 V, 3 GHz	>45 mA	>30 mA
-5V, 10 GHz	>45 mA	>30 mA
0 V, 3 GHz	~18 mA	~14 mA
0 V, 10 GHz	~24 mA	~20 mA

## 4. CONCLUSION

In summary, we have presented a study of a fast MUTC-PD as an OE converter for cryogenic microwave photonic links. The dark current and spectral responsivity of the device were measured at 300 and 80 K. Its RF bandwidth was assessed at -5 V and 0 V bias, and at 300 and 80 K as well. Subsequently, the linearity of the RF output at 3 GHz and 10 GHz was measured up to ~20 dBm optical power, as a function of DC bias voltage and temperature. The experimental results obtained so far form an important stepping stone for the use of highly linear photodiodes for emerging applications in

quantum networking. In future work, we plan to test this device at much colder temperatures ( $\sim 1$  K), as well as with shorter wavelength optical excitations expected to maintain higher responsivities as temperature drops.

## REFERENCES

- [1] S. Pirandola and S. L. Braunstein, “Unite to build a quantum internet,” *Nature* **532**, 169–171 (2016).
- [2] P. Krantz, M. Kjaergaard, F. Yan, T. P. Orlando, S. Gustavsson, and W. D. Oliver, “A quantum engineer’s guide to superconducting qubits,” *Appl. Phys. Rev.* **6**, 021318 (2019).
- [3] A. Morello, J.J. Pla, P. Bertet, and D. N. Jamieson, “Donor spins in silicon for quantum technologies,” *Adv. Quantum Technol.* **3**, 2000005 (2020).
- [4] S. Krinner, S. Storz, P. Kurpiers, P. Magnard, J. Heinsoo, R. Keller, J. Lütolf, C. Eichler, and A. Wallraff, “Engineering cryogenic setups for 100-qubit scale superconducting circuit systems,” *EPJ Quantum Technol.* **6**, 2 (2019).
- [5] J. Yao, “Microwave Photonics,” *J. Lightw. Technol.* **27**, 314–335 (2009).
- [6] V. J. Urick, Jr., J. D. McKinney, and K. J. Williams, *Fundamentals of Microwave Photonics* (Wiley, Hoboken, NJ, 2015).
- [7] F. Lecocq, F. Quinlan, K. Cicak, J. Aumentado, S. A. Diddams, and J. D. Teufel, “Control and readout of a superconducting qubit using a photonic link,” *Nature* **591**, 575–579 (2021).
- [8] Y. M. Zhang, V. Borzenets, N. Dubash, T. Reynolds, Y. G. Wey, and J. Bowers. “Cryogenic performance of a high-speed GaInAs/InP p-i-n photodiode,” *J. Lightw. Technol.* **15**, 529–533 (1997).
- [9] K. Yoshino, Y. Muramoto, T. Furuta, and H. Ito, “High-speed uni-travelling-carrier photodiode module for ultra-low temperature operation,” *Electron. Lett.* **41**, 1030–1031 (2005).
- [10] H. Ito, T. Furuta, S. Kodama, K. Yoshino, T. Nagatsuma, and Z. Wang, “10 Gbit/s operation of uni-travelling-carrier photodiode module at 2.6 K,” *Electron Lett.* **44**, 149–150 (2008).
- [11] Y. Hashimoto, H. Suzuki, M. Maruyama, K. Fujiwara, and M. Hidaka, “40 Gbit/s operation of superconductive single flux quantum digital integrated circuit with optical data input,” *Electron. Lett.* **45**, 87–88 (2009).
- [12] H. Suzuki, “Evaluation of uni-traveling carrier photodiode performance at low temperatures and applications to superconducting electronics,” in *Photodiodes* (J.-W. Shi, ed.) Ch. 2. (IntechOpen, London, 2011).
- [13] A. Beling, X. Xie, and J. C. Campbell, “High-power, high-linearity photodiodes,” *Optica* **3**, 328–338 (2016).
- [14] J. Davila-Rodriguez, H. Leopardi, T. M. Fortier, X. Xie, J. C. Campbell, J. Booth, N. Orloff, S. A. Diddams, and F. Quinlan, “Temperature dependence of nonlinearity in high-speed, high-power photodetectors,” *IEEE Photonics Conference*, paper 8116021 (2017).
- [15] M. Woodson, S. Estrella, E. Fodor, K. Hay, R. P. Stahl, D. Renner, M. Mashanovtich, “An overview of high-power photodiodes for RF applications,” *Proc. SPIE* **11685**, 116850I (2021).

## ACKNOWLEDGEMENTS

A portion of this work was performed at Oak Ridge National Laboratory, managed by UT-Battelle, LLC, for the U.S. Department of Energy under contract no. DE-AC05-00OR22725. Funding was provided by the U.S. Department of Energy (Field Work Proposal ERKJ353).